[14] The already large 6s-6p separation in the atoms Tl and Pb is enhanced in the corresponding cations.
[15] a) H. J. Terpstra, R. A. de Groot, C. Haas, *Phys. Rev. B* **1995**, *52*, 11690; b) G. W. Watson, S. C. Parker, G. Kresse, *Phys. Rev. B* **1999**, *59*, 8481.
[16] A. F. Holleman, N. Wiberg, *Lehrbuch der Anorganischen Chemie*, de Gruyter, Berlin, **1995**.
[17] J. R. Schoonover, T. L. Groy, S. H. Lin, *J. Solid State Chem.* **1989**, *83*, 207.
[18] H. K. Mao, J. Xu, P. M. Bell, *J. Geophys. Res.* **1986**, *91B*, 4673.
[19] M. Evain, *U-Fit: a Cell Parameter Refinement Program*, Institut de Matériaux de Nantes, Nantes, France, **1992**.
[20] R. Letoullec, J. P. Pinceaux, P. Loubeyre, *High Pressure Res.* **1988**, *1*, 77.
[21] M. Thoms, S. Bachau, D. Häusermann, M. Kunz, T. Le Bihan, M. Mezouar, D. Strawbridge, *Nucl. Instrum. Methods Phys. Res. Sect. A* **1998**, *413*, 175.
[22] A. Hammersley, *FIT2D V10.3 Reference Manual V4.0* ESFR, Grenoble, France, **1998**.
[23] A. Boultif, D. Louër, *J. Appl. Crystallogr.* **1991**, *24*, 987.
[24] a) G. Kresse, J. Hafner, *Phys. Rev. B* **1993**, *47*, RC558; b) G. Kresse, J. Furthmüller, *Phys. Rev. B* **1996**, *54*, 11169.
[25] a) D. Vanderbilt, *Phys. Rev. B* **1990**, *41*, 7892; b) G. Kresse, J. Hafner, *J. Phys. Condens. Matter* **1994**, *6*, 8245.
[26] J. Perdew, A. Zunger, *Phys. Rev. B* **1981**, *23*, 5048.
[27] H. J. Monkhurst, J. D. Pack, *Phys. Rev. B* **1976**, *13*, 5188.
[28] P. Blöchl, O. Jepsen, O. K. Andersen, *Phys. Rev. B* **1994**, *49*, 16223.

Solid-Phase Synthesis of Transition Metal Linked, Branched Oligonucleotides**

Ignacio Vargas-Baca, Debbie Mitra, Holly J. Zulyniak, Jay Banerjee, and Hanadi F. Sleiman*

Branched oligonucleotides have recently emerged as attractive synthetic targets for the selective recognition of nucleic acids.[1] These molecules have the potential to act as sensitive diagnostic tools for the detection of DNA sequences,[1a,b] and can specifically bind single-stranded DNA/RNA (antisense/antigene strategy).[1c–e] In addition, they can serve as model complexes for the elucidation of the structure and biological role of branched RNA molecules found in nature.[1a,d] In previous branched systems, the DNA strands were linked together through oligonucleotide or small organic-molecule-based vertices.[1, 2] We recently initiated research into the synthesis and properties of a new class of branched oligonucleotides, in which a transition metal acts as the vertex joining two parallel DNA strands. Transition metal centers come in a range of geometries, coordination numbers, and bond angles that are unavailable in carbon chemistry (e.g., octahedral, square planar, trigonal bipyramidal). By combining this varied coordination chemistry with the highly specific interactions of DNA, we expect that these branched metal–DNA complexes will expand the repertoire of DNA structures to novel motifs.[3] This can be achieved both through their binding to single-stranded DNA and RNA, as well as their self-association and formation of DNA "nanostructures".[2] In addition, the rich redox and luminescence properties of metal centers afford a sensitive marker for detecting and monitoring the association of these new structures.

While many transition metal labeled oligonucleotides were reported recently,[4] the metal center is usually tethered as a pendant functional group on a DNA strand, and hence its geometry cannot influence DNA association.[5] Here we report the first synthesis of a transition metal linked branched oligonucleotide (**1**), in which the DNA strands run parallel to each other and the geometry of the metal center can directly influence the orientation of these strands. Furthermore, we have studied the biological behavior of these branched complexes by hybridization to complementary DNA. Thermal denaturation experiments show the formation of novel transition metal linked DNA duplexes with a stability comparable to that of Watson–Crick A/T duplexes.

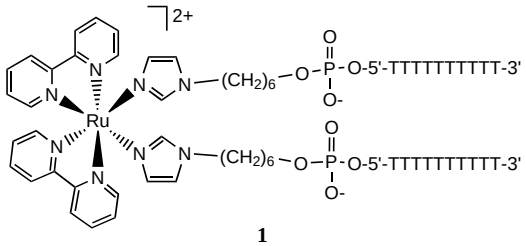

1

In the design of complex **1**, two parallel (5′-3′) oligonucleotide strands are linked to a *cis*-$[(bpy)_2Ru(imidazole)_2]^{2+}$ moiety through *n*-hexyl spacers (bpy = 2,2′-bipyridine). The ruthenium moiety is both redox active and intensely luminescent, and it has been extensively used as a probe of electron transfer processes in proteins.[6] Our convergent solid-phase strategy[7] for the preparation of ruthenium-linked parallel oligonucleotides is outlined in Schemes 1 and 2. This strategy starts with the generation of a ruthenium bis-phosphoramidite branching complex **3**.[8] The reaction of two molar equivalents of 1-(6-hydroxyhexyl)imidazole[9a] with *cis*-$[(bpy)_2Ru(CH_3CN)_2](PF_6)_2$[9b] in refluxing ethanol/water, followed by precipitation with aqueous NH_4PF_6 results in the formation of the *cis*-bis-imidazole ruthenium complex **2** as a deep red solid.[17] The UV/Vis absorption spectrum of **2** shows metal-to-ligand (Ru→bpy) charge transfer (MLCT) bands at 341 and 491 nm.[6a] An interesting feature of this complex is its intense fluorescence, which could prove useful for possible applications as a DNA biosensor. Excitation of the MLCT

[*] Prof. H. F. Sleiman, Dr. I. Vargas-Baca,[+] D. Mitra, H. J. Zulyniak, J. Banerjee
Department of Chemistry, McGill University
801 Sherbrooke St. W., Montreal, Quebec H3A 2K6 (Canada)
Fax: (+1) 514-398-3797
E-mail: hanadi.sleiman@mcgill.ca
[+] Current address:
Department of Chemistry, McMaster University
Hamilton, Ontario L8S 4M1 (Canada)

[**] This work was supported by NSERC (Canada), CFI (Canada) and FCAR (Quebec). The authors gratefully acknowledge Prof. M. J. Damha and his laboratory, McGill University, for helpful discussion.
Supporting information for this article is available on the WWW under http://www.angewandte.com or from the author.

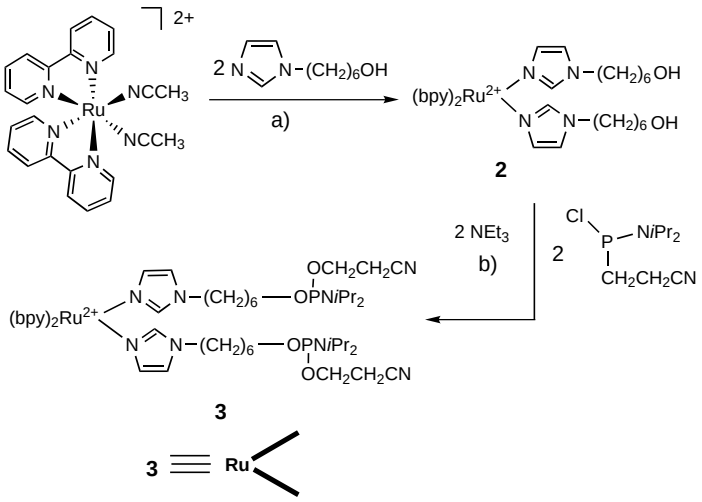

Scheme 1. Synthesis of branching complex **3**. a) Ethanol/water, reflux, 12 h, 86 %; b) CD_2Cl_2, 2 h, quantitative. All complexes are PF_6^- salts.

band at 490 nm in ethanol results in an emission centered at 650 nm.

Complex **2** was functionalized to allow for coupling to DNA by reaction with two molar equivalents of chloro(cyanoethyl)-*N*,*N*-diisopropylphosphoramidite in the presence of triethylamine under an inert atmosphere. The reaction can be monitored by ^{31}P NMR spectroscopy in CD_2Cl_2 and is complete in two hours. The ^{31}P NMR spectrum displays a broad peak at $\delta = 148$ for the phosphoramidite moiety.[10] The bis-phosphoramidite complex **3** is stable in solution at room temperature under an inert atmosphere and was used in the following steps without further purification. One of the attractive features of our conjugation strategy is the compatibility of **3** with the standard protocols for oligonucleotide synthesis. Control experiments on complex **2** showed the stability of the *cis*-$[(bpy)_2Ru(imidazole)_2]^{2+}$ moiety to the conditions of solid-phase DNA synthesis and ammonia cleavage.

In parallel to the synthesis of **3**, the oligonucleotide dT_{10} was assembled on a 500 Å controlled pore glass (CPG) support by using standard solid-phase protocols. To optimize the yield of **1**, our convergent solid-phase strategy requires close proximity of the 5′-OH termini of growing oligonucleotides on the solid support (Scheme 2).[7] Hence, high-density CPG support (56 μmol g^{-1}) was used. Bis-phosphoramidite **3** in CD_2Cl_2 was then added to the solid support under an inert atmosphere, with tetrazole as activator to achieve branching. Subsequent oxidation of the phosphite moiety, cleavage of the oligonucleotide from the solid support in ethanolic ammonia, and evaporation afforded a fluorescent red solid.

The crude mixture was analyzed by denaturing polyacrylamide gel electrophoresis (PAGE) to identify the ruthenium – DNA products (Figure 1 a). The fastest moving band has an electrophoretic mobility identical to that of the control sample of the linear oligonucleotide dT_{10}, and was thus assigned as unmodified DNA. Two slow-moving red fluorescent bands were also visible in the gel. The slowest moving band was attributed to the desired branched ruthenium complex **1** and the next slowest moving band to the mono-

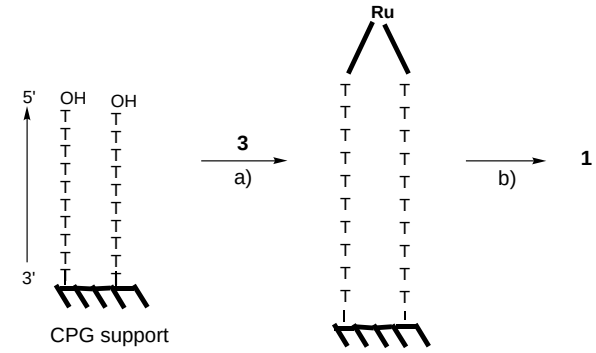

Scheme 2. DNA branching step. a) Tetrazole, RT, 12 h; b) I_2, pyridine, H_2O, then NH_4OH/EtOH, 2 h, RT.

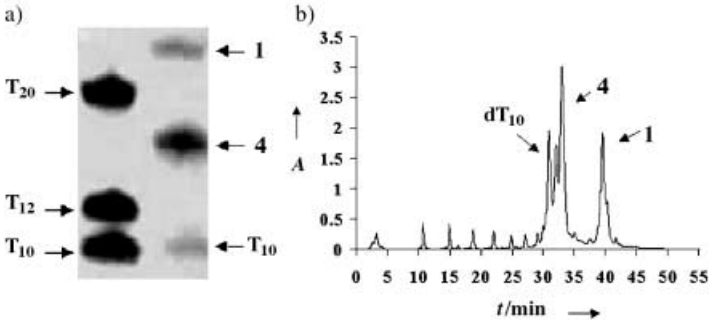

Figure 1. a) Analytical PAGE under denaturing conditions (UV shadowing) of the oligonucleotide mixture obtained according to Scheme 2. b) HPLC (monitoring at 260 nm) of the oligonucleotide mixture. Only the peaks of compounds **1** and **4** show absorbance at 260 and 490 nm. A = absorbance.

stranded ruthenium complex *cis*-$[(bpy)_2Ru^{2+}\{(imidazole)(CH_2)_6O$-5′-$d(T_{10})$-3′$\}\{(imidazole)(CH_2)_6OH\}]$ (**4**; vide infra). The mobility of **1** was significantly lower than that of a 5′-$d(T_{20})$-3′ linear marker, and that of the monostranded complex **4** was lower than that of 5′-$d(T_{10})$-3′, likely due to the presence of the positively charged metal center and the higher molecular weight of these complexes. The intense red color and fluorescence of the ruthenium moiety make it a convenient marker for the identification of the desired ruthenium – DNA complexes.

The products were isolated by ion-exchange HPLC on the crude reaction mixture (Figure 1 b). Monitoring at 260 (DNA π-π* band) and 490 nm (*cis*-$[(bpy)_2Ru(imidazole)_2]^{2+}$ MLCT band) allowed the identification of the fractions containing ruthenium – DNA complexes. Two distinct peaks for such complexes were observed. A MALDI-TOF mass spectrometric analysis of the two isolated samples identified the desired branched ruthenium complex **1** as the fraction with the highest retention time, and the monostranded ruthenium complex **4** as the next-eluting fraction.[11] These results clearly demonstrate the successful synthesis of branched ruthenium – DNA complex **1**, as well as monolabeled complex **4**, by a facile solid-phase approach.

With branched complex **1** in hand, we conducted thermal denaturation experiments[12] to determine its hybridization efficiency with complementary DNA (Figure 2).[13] The melting temperatures were determined for 1:1 and 1:2 mixtures of

  1433-7851/01/4024-4630 $ 17.50+.50/0

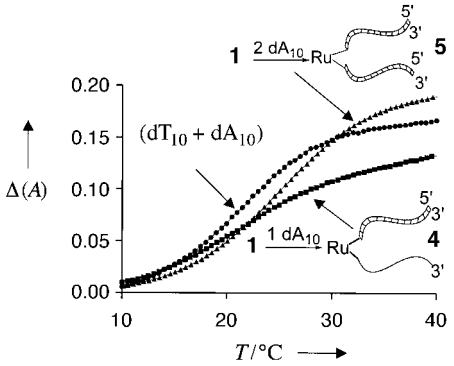

Figure 2. UV absorbance–melting curves at 260 nm. [**1**+dA_{10}] (■); [**1**+2dA_{10}] (▲); (dA_{10}+dT_{10}) (●). Normalized change in absorbance, $\Delta(A)$, was calculated by using $(A_t - A_0)/A_f$, where A_t is the absorbance at a given temperature, A_f is the final absorbance at 90 °C, and A_0 is the initial absorbance at 5 °C. The melting temperatures were calculated to be the maxima of the first derivative plot of the melting curves at 260 nm. % H was calculated using the formula $100[(A_f - A_0)/A_f]$.[1d] The buffer system used was 140 mM KCl, 5 mM Na_2HPO_4, and 1 mM $MgCl_2$, pH 7.2.

1 and dA_{10}. The results for the 1:1 ratio indicated the formation of a duplex involving one of the strands of the branched complex. The thermal denaturation curve at 260 nm showed a monophasic transition at 22.1 °C with a hyperchromicity of 13%. These results are promising as they coincide with the melting temperature of 21.0 °C for a Watson–Crick dA_{10}/dT_{10} duplex in the same buffer system (hyperchromicity 17%). With two equivalents of dA_{10}, a monophasic transition was observed at 26.0 °C with a hyperchromicity of 17%.[14] These results are consistent with hybridization of both strands of **1** and formation of a novel complex **5** (Figure 3), in which a transition metal moiety links two DNA duplexes. Indeed, molecular modeling studies on **5**[15] predict no significant steric or energetic barrier to the formation of this structure (Figure 3). Further characterization of the hybridized complexes by nondenaturing gel electrophoresis and CD spectroscopy is currently underway.

In conclusion, we have prepared the first branched DNA structure **1** containing a transition metal center as the branch point, to which two oligonucleotide strands are attached through monodentate ligands. Importantly, the convergent solid-phase synthesis of **1** allows for the possible incorporation of a range of metal complexes, spacers between the metal atom and DNA, and DNA sequences into the structure.[16] Complex **1** is expected to perform a dual role. It contains luminescent and redox-active *cis*-$[(bpy)_2Ru(imidazole)_2]^{2+}$ that is incorporated into the oligonucleotide and thus can potentially act as a DNA hybridization probe.[4] In addition, analogues of complex **1** containing mixed DNA sequences are expected to associate with their complementary partners to generate a new class of DNA nanostructures. The pioneering work of Seeman[2a] and other recent contributions[2] have elegantly demonstrated the exciting promise of DNA as a building block for nanotechnology. Complexes such as **1** allow the metal-mediated self-assembly of DNA into a new class of photo- and electroactive DNA nanostructures. We are currently investigating the fluorescence response of these complexes to DNA hybridization, as well as their potential for the construction of higher order DNA structures.

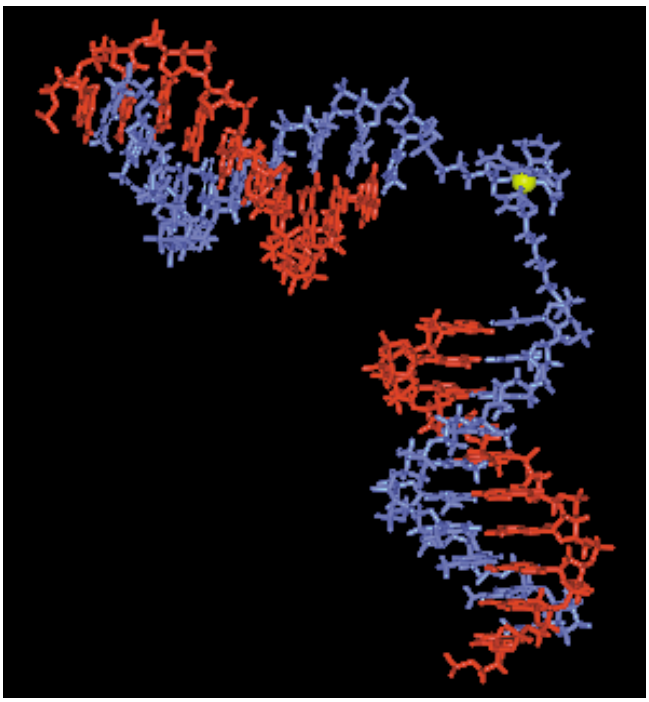

Figure 3. Optimized structure of the expected ruthenium-linked bis(double helical) DNA complex **5**, calculated as a local minimum by the AMBER force-field method.[15] The branched ruthenium complex **1** is shown in blue (ruthenium atom in yellow), and the two dA_{10} strands are shown in red. Because of the flexibility of the hexyl spacer, as well as the influence of solvent and counterions, the structure shown may not be a unique conformation of complex **5**.

Received: July 6, 2001 [Z17443]

[1] a) R. S. Braich, M. J. Damha, *Bioconjugate Chem.* **1997**, *8*, 370–377; b) T. Horn, C. Chang, M. Urdea, *Nucleic Acids Res.* **1997**, *25*, 4835–4841; c) D. Praseuth, A. L. Guieysse, C. Helene, *Biochim. Biophys. Acta* **1999**, *1489*, 181–206; d) R. H. E. Hudson, A. H. Uddin, M. J. Damha, *J. Am. Chem. Soc.* **1995**, *117*, 12470–12477, and references therein; e) M. D. Sorensen, M. Meldgaard, V. K. Rajwanshi, J. Wengel, *Bioorg. Med. Chem. Lett.* **2000**, *10*, 1853–1856, and references therein.

[2] a) N. C. Seeman, *Annu. Rev. Biophys. Biomol. Struct.* **1998**, *27*, 225–248; b) J. J. Storhoff, C. A. Mirkin, *Chem. Rev.* **1999**, *99*, 1849–1862; c) R. P. Fahlman, D. Sen, *J. Am. Chem. Soc.* **1999**, *121*, 11079–11085; d) J. Shi, D. E. Bergstrom, *Angew. Chem.* **1997**, *109*, 70–72; *Angew. Chem. Int. Ed. Engl.* **1997**, *36*, 111–113; e) M. S. Shchepinov, K. U. Mir, J. K. Elder, M. D. Frank-Kamenetskii, E. Southern, *Nucleic Acids Res.* **1999**, *27*, 3035–3041; f) M. Scheffler, A. Dorenbeck, S. Jordan, M. Wustefeld, G. von Kiedrowski, *Angew. Chem.* **1999**, *111*, 3514–3518; *Angew. Chem. Int. Ed.* **1999**, *38*, 3312–3315; g) S. M. Waybright, C. P. Singleton, K. Wachter, C. Murphy, U. H. F. Bunz, *J. Am. Chem. Soc.* **2001**, *123*, 1828–1833.

[3] Metal-mediated self-assembly of peptide structures: a) M. R. Ghadiri, C. Soares, C. Choi, *J. Am. Chem. Soc.* **1992**, *114*, 825–831; b) K. Suzuki, H. Hiroaki, D. Kohda, H. Nakamura, T. Tanaka, *J. Am. Chem. Soc.* **1998**, *120*, 13008–13015.

[4] a) D. J. Hurley, Y. Tor, *J. Am. Chem. Soc.* **1998**, *120*, 2194–2195; b) H. S. Joshi, Y. Tor, *Chem. Commun.* **2001**, 549–550; c) S. I. Khan, A. E. Beilstein, M. W. Grinstaff, *Inorg. Chem.* **1999**, *38*, 418–419, and references therein; d) K. Tanaka, M. Tasaka, H. Cao, M. Shionoya, *Eur. J. Pharm. Sci.* **2001**, *13*, 77–83; e) E. Meggers, P. L. Holland, W. B.

  1433-7851/01/4024-4631 $ 17.50+.50/0

Tolman, F. E. Romesberg, P. G. Shultz, *J. Am. Chem. Soc.* **2000**, *122*, 10714 – 10715.
[5] Three reports have described systems containing branched/difunctional oligonucleotides and metal centers; however, none of these systems has a metal center whose geometry directly influences the orientation of the DNA strands. a) S. Takenaka, Y. Funatu, H. Kondo, *Chem. Lett.* **1996**, 891 – 892; b) F. D. Lewis, S. A. Helvoigt, R. L. Letsinger, *Chem. Commun.* **1999**, 327 – 328; c) see ref. [2g].
[6] a) K. B. Reddy, M. P. Cho, J. F. Wishart, T. J. Emge, S. S. Isied, *Inorg. Chem.* **1996**, *35*, 7241 – 7245; b) T. Pascher, J. R. Winkler, H. B. Gray, *J. Am. Chem. Soc* **1998**, *120*, 1102 – 1103.
[7] M. J. Damha, K. Ganeshan, R. H. E. Hudson, S. V. Zabarylo, *Nucleic Acids Res.* **1992**, *24*, 6565 – 6573.
[8] Selected spectroscopic data of complex **2**: ^{1}H NMR (400 MHz, [D$_6$]acetone): $\delta = 0.85$ (m, 4H), 1.10 (m, 4H), 1.25 (m, 4H), 1.55 (m, 4H), 3.30 (t, 4H), 3.90 (t, 4H), 6.80 (s, 2H), 7.18 (br s, 2H), 7.32 (t, 2H), 7.72 (t, 2H), 7.82 (br s, 2H), 7.89 (t, 2H), 8.10 (m, 4H), 8.45 (d, 2H), 8.54 (d, 2H), 9.13 (d, 2H). FAB-MS: *m*/*z*: 894.9 [$M - PF_6$].
[9] a) K. Iizuka, K. Akahane, Y. Kamijo, D. Momose, Y. Ajisawa, *Brit. UK Pat. Appl.* **1979**, GB 2016452; b) G. M. Brown, R. W. Callahan, T. J. Meyer, *Inorg. Chem.* **1975**, *14*, 1915 – 21.
[10] The expected diastereomers from the chirality of both the *cis*-[(bpy)$_2$Ru(imidazole)$_2$]$^{2+}$ and the phosphoramidite groups could not be resolved at 200 MHz.
[11] Complex **1**: HPLC: 22% of the mixture, MALDI-TOF MS: *m*/*z*: 6861 [M+2Na$^+$]. Complex **4**: HPLC: 54% of the mixture, MALDI-TOF MS: *m*/*z* 3914 [M+2Na$^+$+Li$^+$].
[12] The buffer system used was 140 mM KCl, 5 mM Na_2HPO_4, and 1 mM $MgCl_2$, pH 7.2. This buffer is known to inhibit the formation of a DNA triple helix, which could arise from the association of **1** with one strand of dA_{10}.[1d]
[13] In parallel, control experiments on complex **2** established that the *cis*-[(bpy)$_2$Ru(imidazole)$_2$]$^{2+}$ moiety is stable to the high temperatures required in the melting experiments.
[14] The origin of the observed increase in stability of the duplexes in **5**, as compared to natural dA_{10}/dT_{10} duplexes, is still under investigation. Thermal denaturation studies on monostranded complex **4** with dA_{10} showed a similar increase in T_m,[17] and this suggests that the enhanced stability of the DNA duplexes in these structures may be due to the positively charged metal center. In this respect, the decrease in T_m and hyperchromicity observed for complex **1** with 1 equiv of dA_{10} relative to 2 equiv dA_{10} is also under investigation.
[15] Assuming B-form DNA and fixing the coordinates of the ruthenium moiety according to a reported crystal structure of *cis*-[(bpy)$_2$Ru(imidazole)$_2$]$^{2+}$,[6a] calculations were performed with Hyperchem 6, Hypercube, FL (USA).
[16] Current efforts are focused on the synthesis of analogues of **1** with rigid spacers between imidazole ligands and DNA strands, so that the geometry of the metal center can directly influence the orientation of the strands.
[17] See Supporting Information for experimental details on the synthesis and characterization of complexes **1** – **4**, as well as thermal denaturation studies.

The Mechanism of Hydroamination of Allenes, Alkynes, and Alkenes Catalyzed by Cyclopentadienyltitanium – Imido Complexes: A Density Functional Study**

Bernd F. Straub* and Robert G. Bergman*

Considerable effort has been directed towards the development of procedures for hydroamination across carbon – carbon multiple bonds, and several catalytic systems for allene, alkyne, and alkene hydroamination have been investigated.[1] However, a general catalyst for the hydroamination of nonactivated unsaturated hydrocarbons remains elusive. A catalyst for the selective anti-Markovnikov addition of amines to terminal alkenes would be of particular interest [Eq. (1)].

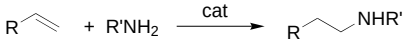

(1)

Recent kinetic studies have been carried out to elucidate the mechanism of hydroamination catalyzed by cyclopentadienyltitanium complexes[2–5] such as the dimethyltitanocene **1** and the imido complex **2a** (Scheme 1).[4, 5] Formation of the active monocyclopentadienyltitanium – imido species [CpTi=NR(NHR)] **3a** (R = 2,6-Me$_2$C$_6$H$_3$) from both the pyridine adduct **2a** and the precatalyst **1** has been established (Scheme 1).[4]

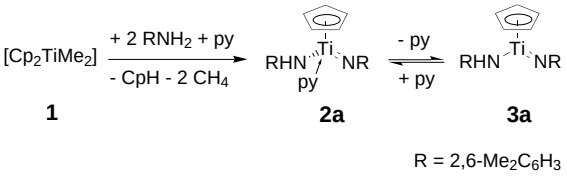

Scheme 1. Generation of [CpTi=NR(NHR)] **3a** from precatalyst [Cp$_2$TiMe$_2$] (**1**) and by equilibration with [CpTi=NR(NHR)py] **2a**.[4]

Titanaazacyclobutenes and titanaazacyclobutanes are proposed as intermediates in the catalytic cycle,[2a, 4, 5] in analogy to the [Cp$_2$Zr(NHR)$_2$]-catalyzed hydroamination of alkynes[6] or the stoichiometric reaction of allenes with zirconium and titanium pyridine imido derivatives.[7] However, the mechanism of the protonation of the titanacycle by the amine is not well understood. Here we report high-level density functional model calculations on the intermediates involved in this step. The origin of the differences between the activation barriers

[*] Dr. B. F. Straub, Prof. R. G. Bergman
Department of Chemistry
University of California
Berkeley, CA 94720-1460 (USA)
Fax: (+1) 510-642-7714
E-mail: bergman@cchem.berkeley.edu
bfstraub@uclink.berkeley.edu

[**] This work was supported by the US National Institutes of Health (grant no. GM-25459 to R.G.B.). B.F.S. gratefully acknowledges a Feodor Lynen research fellowship of the Alexander von Humboldt foundation.

Supporting information for this article is available on the WWW under http://www.angewandte.com or from the author.

  1433-7851/01/4024-4632 $ 17.50+.50/0